Image Cover Sheet

CLASSIFICATION	SYSTEM NUMBER
UNCLASSIFIED	143069

TITLE

FLIGHT TEST OF A CYLINDRICAL TOWBODY FOR AN AIRBORNE SQUID GRADIOMETER

System Number:

Patron Number:

Requester:

Notes:

DSIS Use only:

Deliver to: JR

Defence Research Establishment Pacific
Centre de recherches pour la defense pacifique

DEFENCE RESEARCH ESTABLISHMENT PACIFIC

CFB Esquimalt, FMO, Victoria, B.C. V0S 1B0

Technical Memorandum 94-16

FLIGHT TEST OF A CYLINDRICAL TOWBODY FOR AN AIRBORNE SQUID GRADIOMETER

Harold Wilson, David Hopkin,
Brian Dunstan and J. Bradley Nelson

March 1994

Approved by:

Chief

Canada

Research and Development Branch
Department of National Defence

Abstract

The Magnetic Anomaly Detection Group at DREP is studying the feasibility of using SQUID magnetic gradiometers in airborne antisubmarine warfare. As part of this project, a non-magnetic towbody has been built to carry a vertical gradiometer in an airborne trial of SQUID systems. The towbody is essentially a circular cylinder with the air flow perpendicular to the cylinder axis. We describe the characteristics of the towbody that were observed during a flight test. The results presented include drag, static pitch, towbody oscillations and acceleration spectra. We conclude that the towbody can be used for a trial of a gradiometer.

Résumé

Le Group de détection d'anomalies magnétiques au CRDP étudie la faisabilité d'utiliser des gradiomètres magnétiques SQUID dans la guerre contre les sous-marins exécuté au moyen des dispositifs aéroportés. Pour ce projet nous avons fait construire un corps remorqué non magnétique pour transporter un gradiomètre vertical dans un essai aéroporté du systèmes SQUID. Le corps remorqué consiste essentiellement en un cylindre circulaire dont le mouvement d'air est perpendiculaire à l'axe du cylindre. Nous décrivons les caractéristiques du corps remorqué observées durant un vol d'essai. Les résultats que nous présentons comprennent le force de traînée, le tangage statique, l'oscillations du corps remorqué, et les spectres d'accélération. Nous concluons que le corps remorqué peut servir pour l'essai d'un gradiomètre.

1. Introduction

The Magnetic Anomaly Detection (MAD) Group at DREP is studying the feasibility of using superconducting (SQUID) magnetic gradiometers in airborne antisubmarine warfare. As part of this project, a non-magnetic towbody has been developed to carry a small test gradiometer in a preliminary airborne trial of superconducting systems. This report describes the flight characteristics of the towbody which were observed during the second trial of the towbody at AETE, CFB Cold Lake in November 1993.

Ref. 1 discusses the background for this project as well as the mechanical design and aerodynamic calculations of the towbody and the results of the first trial. The towbody is shown in Fig. 1. Because the towbody is intended to carry a SQUID gradiometer in a vertical dewar, it has an unusual shape : it is a circular cylinder with air flow perpendicular to the axis. The towbody is carried on the end of a long rope so that it is well removed from magnetic and RF interference of the towing helicopter.

The first trial revealed a pitching instability when the airspeed reached 60 knots in level flight. Accelerometers and magnetometers aboard the towbody showed that the pitching amplitude reached ±14° at ~0.7 Hz within 4 sec of the start of the unstable motion. The initial trial also showed that the towbody drag was much higher than expected.

Analysis of the data from the trial did not reveal the cause of the pitch instability. It was clear that the problem was associated with the severe forward pitch of the towbody at high speeds, but the detailed mechanism of the motion and the source of the driving forces was unknown. Consequently, it was decided to test the towbody in a water tank at the Institute for Marine Dynamics (IMD) in St. John's, Nfld. These tests were done in March 1993 at speeds up to 2.5 m/s where the Reynolds number is the same as at 53 knots in air. The trials at IMD showed that the high drag was caused by 1-cm high strakes which had been added to prevent coupling between vortex shedding from the towbody and side-to-side pendulum motion. The high drag also caused the pitch forward which led to the instability. The data from the water-tank experiments are discussed in Section 2.

Section 3 describes the modifications which were made to the towbody to prepare it for the second flight trial at AETE. These changes were intended to reduce the forward pitch.

The flight trials are outlined briefly in Section 4 and the data analysis and flight characteristics are given in Section 5.

Section 6 presents the conclusions drawn from the flight trial.

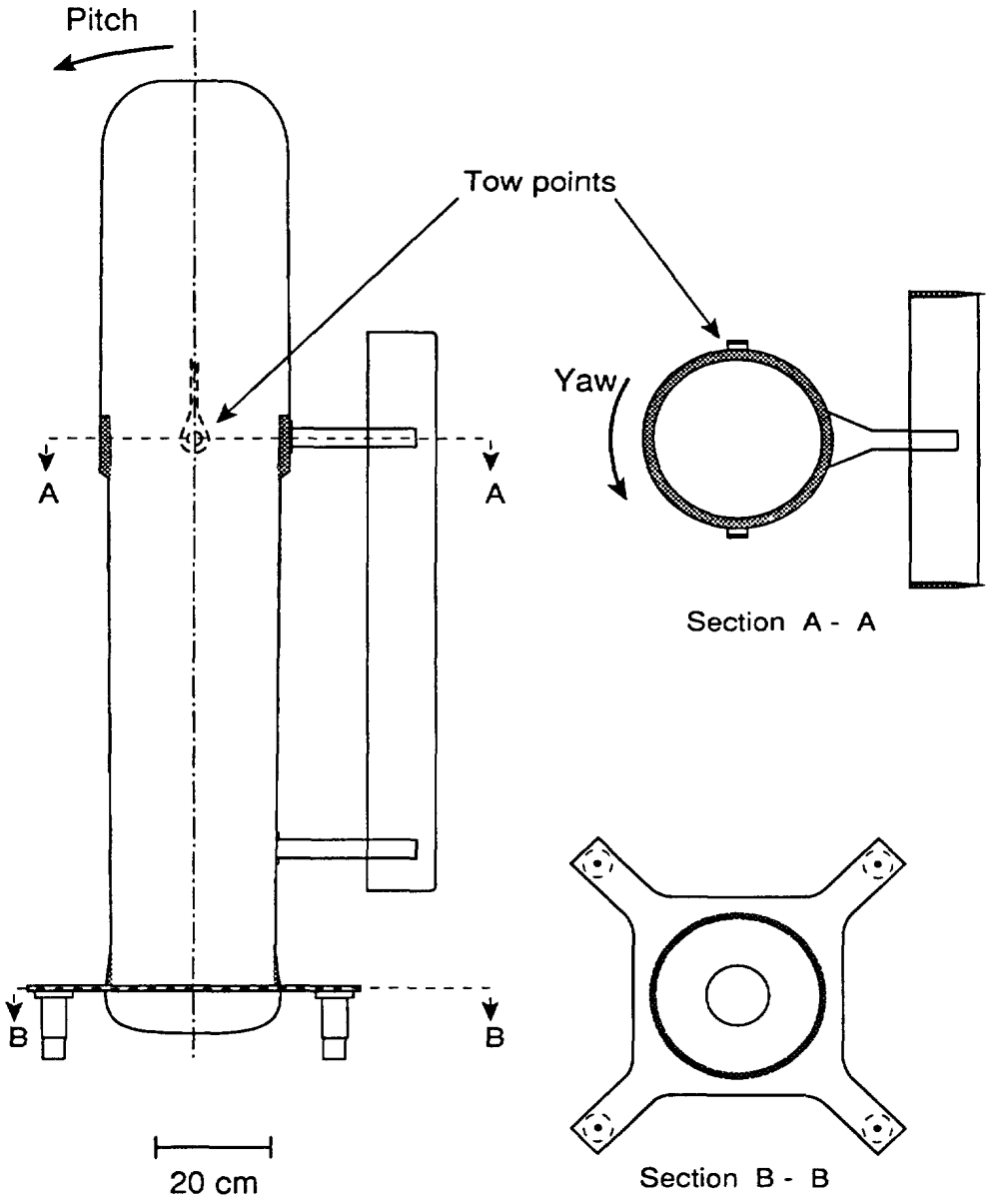

Figure 1. An outline sketch of the towbody tested in the flight trials.

2. Water-Tank Tests

The towbody modifications required for the water-tank tests at IMD were minor. A mounting bracket with a load cell for measuring forces and moments was installed inside of the towbody and a 10-cm hole was cut in the back of the towbody to attach a mounting arm to the load cell.

The theory of hydrodynamics shows that the flow of a fluid around a body can be characterized by the Reynolds number

$$Re = vD/\nu \qquad (1)$$

where v is the fluid speed, D is a characteristic size of the body (in this case the cylinder diameter), and ν is the kinematic viscosity. The kinematic viscosity of air is $\nu = 1.45 \times 10^{-5} m^2/s$ while the kinematic viscosity of water is $\nu = 1.32 \times 10^{-6} m^2/s$, so the Reynolds number in air is the same as the Reynolds number in water when

$$\frac{v(air)}{v(water)} = \frac{\nu(air)}{\nu(water)} = 11 \quad .$$

Hydrodynamic forces and moments on the towbody in a fluid with density ρ and speed v are given by

$$F = \frac{\rho v^2}{2} S \times C(Re) \qquad (2)$$

where factor S is the towbody area perpendicular to the flow and C(Re) is the dimensionless force coefficient and is a function of the Reynolds number only. To calculate the aerodynamic force on the towbody, the force in water is measured at the same Reynolds number, eq. (2) is used to calculate C and then (2) is used again to get the force in air.

The results of the tests at IMD are discussed below.

(i) Drag, Pitching Moment, and Errors

Table I lists the measurements of the drag and pitching moment of the towbody at a range of water speeds. Measurements were made with 1-cm strakes mounted on the lower part of the towbody (as in the first flight trial at AETE) and were then repeated with the strakes removed. The centre-of-drag is also given in cm below the tow point. All of the results are for a towbody with pitch=0 and yaw=0.

An examination of all of the data from the water-tank tests suggests that the force measurements have a random error of ~9 N and the moment error is ~4 N·m, but as we note below, there may be a large unknown systematic error in the load-cell data.

Table I. Drag and pitching moments at pitch=0, yaw=0. The moments and centre of drag are given relative to the point where the tow rope is attached to the body. Positive moment pitches the top of the towbody forward and the centre of drag is given in cm below the tow point.

Water speed (m/s)	Re	Strakes ON Drag (N)	Strakes ON Moment (N·m)	Strakes ON C-of-D (cm)	Strakes OFF Drag (N)	Strakes OFF Moment (N·m)	Strakes OFF C-of-D (cm)
1.0	2.7×10^5	225	60	27.5	165	45	27.5
1.5	4.1 "				335	105	30.5
2.0	5.5 "	830	250	30.0	590	185	31.5
2.5	6.8 "				925	290	31.5

The data shown in Table I are somewhat surprising because the centre of drag did not move significantly when the strakes were removed. This indicates that the combined centre of drag of the top of the towbody, the feet and bottom plate, and the tail was close to the centre of drag of the lower part of the towbody with or without strakes.

For water speeds in the range 1.5-2.5 m/s (corresponding to air speeds of 32-54 knots and Reynolds numbers of $4\text{-}7.0\times10^5$) and with no strakes on the towbody, the drag coefficient C_D (eq. (2)) is constant with the value

$$C_D = 0.49 \ .$$

(The towbody cross section is $S=0.606\ m^2$). This is a low value of the drag coefficient. Fig. 2 shows that $C_D<0.7$ for $Re>4\times10^5$ can be achieved only with surface roughness $<1\times10^{-3}$, at least for very long cylinders. For a cylinder diameter of D=36 cm, this means a roughness of only 0.3 mm. Fig. 2 also shows that a constant value of C_D at $Re=4\times10^5$ is inconsistent

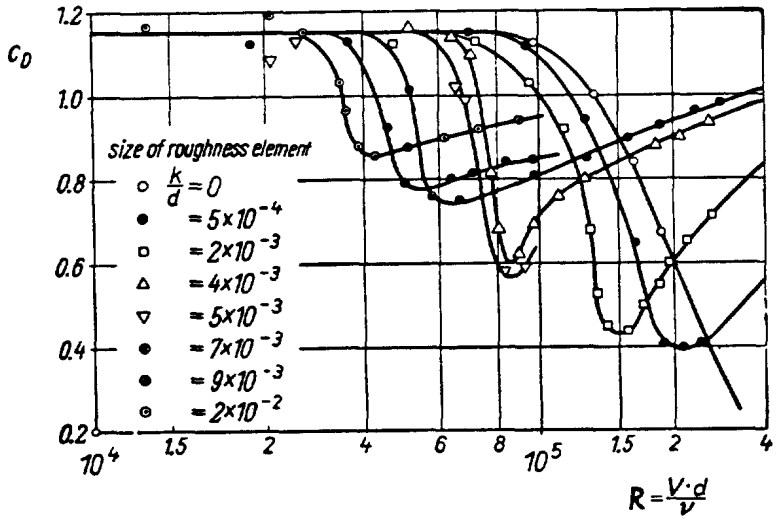

Figure 2. Drag coefficient for rough circular cylinders. (Ref. 2, Fig. 21.18).

with surface roughness $<1\times10^{-3}$. For the range $Re=4\text{-}7\times10^{5}$, a constant C_D is expected only with surface roughness $>3\times10^{-3}$ which should yield a minimum drag coefficient of ~0.8.

It is hard to estimate the effects of the bottom plate, feet, tail and tow-rope attachments (which result in greater roughness and higher drag), and the rounded top and finite length:diameter ratio (which lower it). Ref. 3 shows the effect of length:diameter ratio on C_D just below the transition to turbulent flow for smooth circular cylinders ($Re=9\times10^{4}$). At this speed, C_D of a cylinder with a length:diameter ratio of 6 is only 65% of C_D of an infinitly long cylinder. How this effect combines with the rapidly-varying C_D in the transition region is unclear, and the best we can do is guess that the finite length of the towbody should reduce the drag coefficient by up to 65% of the C_D displayed in Fig. 2. Thus the low C_D by itself may not indicate a measurement error.

Comparison with the flight data reported in Ref. 1 does indicate a problem. Ref. 1 concluded that the drag coefficient was ~1.2±0.1 at 50 knots air speed ($Re=6.5\times10^{5}$), but the uncertainty in the tow-rope angle was probably underestimated, so a better value is $C_D=1.2\pm0.2$.

Table I shows that, at both 1.0 and 2.0 m/s, the 1-cm strakes on the towbody raised the total drag by ~40%. Ref. 1 (Section IV(c)) wondered why the drag was so high. The answer is partly that the strakes were so large that the lower part of the towbody acted more like a flat plate than a cylinder. However, at 2.0 m/s, with strakes, $C_D=0.68$ which is still significantly below the value of C_D~1.2±0.2 from the flight trial. This conclusion does not depend on details of surface roughness and the uncertain drag of a finite cylinder in the transition from laminar to turbulent flow.

Section 5(iii) below shows that a similiar discrepancy was observed in the second flight test, where the drag coefficient with small strakes and also with no strakes was $C_D=0.70\pm0.05$ for $Re=0.8\text{-}1.1\times10^{6}$, while the water tank result is $C_D=0.49$.

We conclude that either there is an error in the water-tank data, or that the forces did not scale according to equation (2) because the towbody configuration was slightly different in the flight trial where a bridle of 6-mm rope attaches the towbody to the tow rope.

The fact that the pitching moments made some sense anyway suggests that, if there was an error in the water-tank data, all of the load-cell outputs had the similar errors.

(ii) Effect of towbody pitch

The drag, lift and pitching moment of the towbody were measured at a water speed of 2 m/s with pitch angles ψ between -10° and +10° ($\psi>0$ when the top of the towbody is pitched forward). Three configurations were tested : (1) strakes on, tail on; (2) strakes off, tail on and (3) strakes

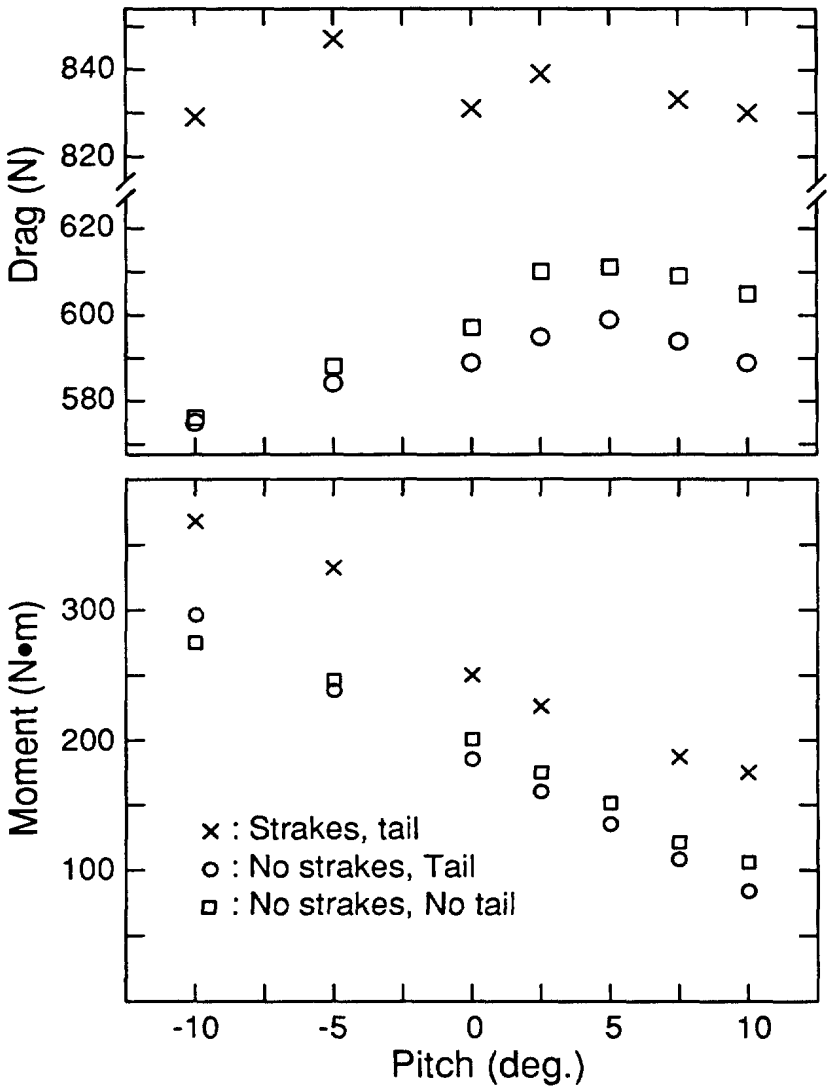

Figure 3. Drag and pitching-moment measurements at 2.0 m/s water speed. Positive moment pitches the top of the towbody forward. No attempt has been made to correct systematic errors in the data.

off, tail off. (The tail was removed for one of the runs so its righting moment could be measured.) Fig. 3 shows the reported drag and pitching moments referred to the tow-rope attachment point. No attempt has been made to correct the systematic error discussed above.

Towbody pitch has only a small effect on total drag, at least for pitch angles in the range $-10° < \psi < 10°$.

Comparison of the pitching moments with the tail on and off shows that the tail provides only a small righting moment. At 10° pitch forward, the tail lift is ~-60 N. The tail is mounted 0.46 m behind the tow point, so the tail lift provides only -25 N·m of pitching moment while the drag of

the towbody provides a moment of +105 N·m with the strakes off and +175 N·m with strakes on.

The horizontal tail surfaces have such a small lift and moment because they are sitting in the towbody's turbulent wake. In order to provide a useful pitching moment, the tail surfaces must be mounted above the top of the towbody or else must extend farther to the side.

Fig. 3 also shows that the tail's drag is a negligible part of the total drag. In fact, the data suggest a higher drag with the tail off. This is impossible, so we conclude that there are systematic errors of ~10 N in the drag measurements from the water-tank tests, in addition to the systematic calibration error.

3. Modifications to the towbody

The first trial showed that the towbody had a pitch instability when it pitched forward to ~15°. The water-tank trials at IMD which were discussed in Section 2 showed that the large pitch forward resulted from the high drag of the strakes and from the inability of the tail to provide a righting moment because it sits in the turbulent air behind the towbody.

Three modifications were made to the towbody in an effort to reduce the pitch-forward problem :

(i) A weight was added at the bottom of the towbody. In the first flight trial, the total towbody weight was 83 kg and the centre of gravity was 24 cm below the tow point. A 13.6-kg weight was added at the bottom (99 cm below the tow point), increasing the total weight to 97 kg and lowering the centre of gravity to 35 cm below the tow point. Before the change, the gravitational righting moment at pitch ψ was

$$M(\text{gravity}) = (3.44\ \text{N·m/deg}) \times \psi \ .$$

Adding the weight increased the righting moment to

$$M(\text{gravity}) = (5.75\ \text{N·m/deg}) \times \psi \ .$$

The added weight also increased the moment of inertia about the pitch axis from $I=19.4\ \text{kg·m}^2$ to $33.0\ \text{kg·m}^2$. The predicted natural frequency for rocking around the pitch axis was unchanged at ~0.5 Hz.

(ii) Strakes were left off the towbody. The water-tank results showed that this should reduce the aerodynamic pitching moment by 25% at $\psi=0°$ and by 40% at $\psi=7.5°$, at least for air speeds up to 50 knots.

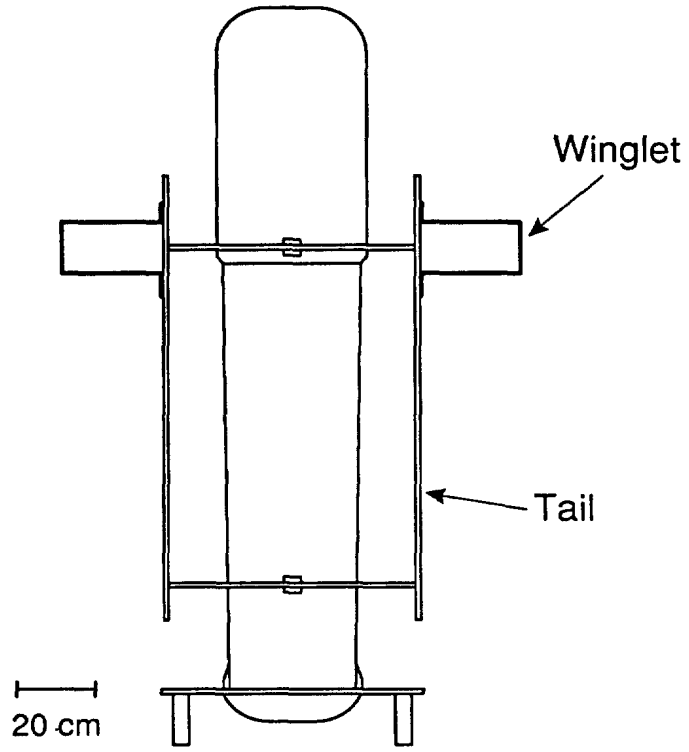

Figure 4. Rear view of the towbody showing the winglets mounted on the tail.

(iii) Small winglets were added on the outside of the tail as shown in Fig. 4. While calculations showed that the pitch should remain below 10° with no additional tail lift up to speeds of ~90 knots, it was decided that small winglets should be added to try to keep $\psi<8°$.

The winglets shown in Fig. 2 form a pair of small-aspect-ratio wings in a 'boxplane' configuration. The wings are 25 cm in length, the span is 14 cm and the wing separation is 13 cm. The lift of such wings is discussed in Ref. 4 (Chap. 17, Sec. 1 and in Chap. 20, Sec. 2). The estimated lift of the wing pair at pitch ψ and speed v is

$$F = [1.03\times10^{-3}\ \mathrm{N/(deg\cdot knot^2)}]\times v^2\psi \quad . \qquad (3)$$

Eq. (3) is only an estimate. First, it is hard to predict the performance of short-aspect-ratio wings. Second, this is not a perfect boxplane because the vertical tail on one side extends well above and below the winglets and it must disturb the airflow. Third, the winglets are made of sheet aluminum and the sharp edges could lead to separated airflow at lower speeds than expected. Nevertheless, (3) should provide a guide to the performance of the winglets. At 80 knots, the winglets should provide a

righting moment of

$$M(\text{winglet}) = F \cdot (0.46\text{m}) = (3.0\ \text{N}\cdot\text{m/deg}) \times \psi \qquad (4)$$

which will reduce the towbody pitch by 35%.

4. The Flight Trials

The second flight trial was performed at AETE in November 1993. The flights were basically the same as the flights reported in Ref. 1. A CH-135 ('Twin Huey') helicopter was used to tow the towbody on a 24-m long 6-mm diameter kevlar tow rope. A heavy 4-m 'pendant' was used to connect the towrope to the helicopter and a bridle connected the tow rope to the towbody, so the towbody was carried 29 m below the helicopter. Videotapes and still photographs of the towbody were recorded by a photographer in a CH-136 ('Kiowa') chase helicopter.

The motion-sensing instrumentation was identical to that used in the first trial (see Ref. 1, Section III). It consisted of a three-axis accelerometer and a three-axis magnetometer mounted in the towbody. The sensor signals were transmitted to the helicopter via optical fibre where they were recorded by a small computer. The instrumentation worked flawlessly except for data errors which occur every 5.00 sec in the vicinity of the runways at CFB Cold Lake and are caused by interference from a radar at the airport. A precise calibration of the accelerometers and magnetometers was performed using the Helmholtz coils and rocker facility and DREP's magnetometer test site near Victoria.

The pickup and landing procedures were the same as in the previous trial. A crew member looked out the door of the helicopter and instructed the pilot which way to move the aircraft so that the tow rope did not pull the towbody over, but also did not become so slack that it could flap in the downwash. The takeoffs and landings were done without mishap in all three flights.

The towbody stability was tested in level flight and in climbs and descents of 500 ft/min and 1000 ft/min at speeds from 20 to 80 knots. The towbody was stable in all conditions. After establishing stability, straight and level flights were done to get data for spectral analysis of the magnetometer and accelerometer signals.

Three slightly different configurations were used. In the first flight, there were no strakes on the towbody and the winglets described above were mounted in the tail. In the second, the winglets were removed. For the third flight, small strakes were placed on 60% of the sides of both the lower and upper parts of the towbody. The strakes consisted of a bead of silicone adhesive and were ~2.5 mm thick on the lower part of the towbody and ~1.5 mm thick on the upper part.

5. Test results

The towbody accelerometers were analyzed to determine the pitch angle and the acceleration spectra. The vector magnetometer gave the amplitudes of pitch, yaw and roll motions. Analysis of the photographs taken by the chase aircraft gave the tow-rope angle and the towbody drag.

Analysis of the data showed that the axes of the vector magnetometer and the vector accelerometer were closely aligned with the towbody axes ($\hat{e}_1$='right', $\hat{e}_2$='forward', $\hat{e}_3$='up'). The acceleration and magnetic field vectors were calculated relative to the towbody axes by rotating the measured data by 2.5°.

(i) Towbody Pitch

In straight flight, the zero-frequency output of the acceleration along the 'forward' direction of the towbody is given by

$$A_2 = -g\sin\psi \qquad (5)$$

where ψ is the pitch angle ($\psi>0$ when the top of the towbody pitches forward). Figure 5 shows the pitch in the three configurations tested.

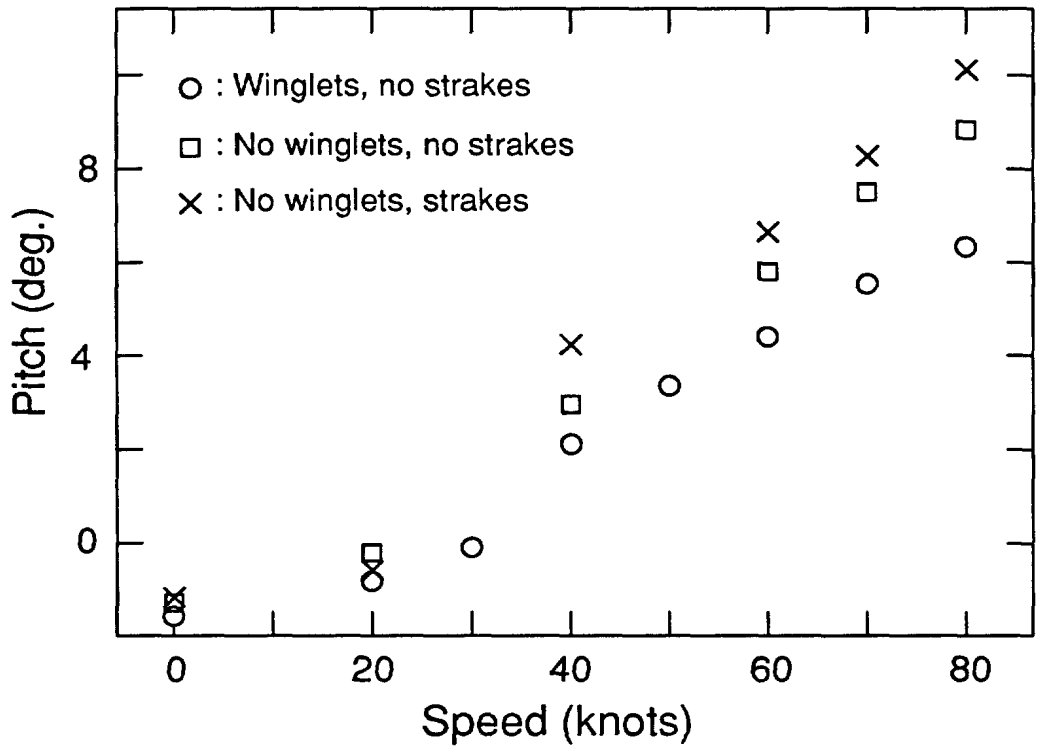

Figure 5. Towbody pitch angle at speeds up to 80 knots measured by the 'forward' accelerometer.

The winglets reduced the forward pitch from 8.82°±0.13 to 6.31±0.21° The estimate of winglet lift given above predicted a pitch reduction from 8.8° to 5.7°, so the winglet lift was 81±8% of the estimated value.

The small strakes added in the third flight caused a significant increase in pitch at speeds above 40 knots. At 80 knots, the pitch rose from 8.82±0.13° to 10.11±0.26° which required an increase in the aerodynamic pitching moment of 7.4±1.7 N·m. If it is assumed that the drag increased evenly over the whole length of the towbody, then the centre of the change in drag would be 0.19 m below the tow point and the total drag increase is 39±9 N. The drag results discussed in the next part of this section indicate that the situation is more complicated because, in fact, the small strakes did not increase the total drag.

We conclude that the severe pitch forward problem reported in Ref. 1 was caused by the heavy strakes on the lower part of the towbody which increased the aerodynamic pitching moment, by insufficient weight at the bottom which reduced the gravitational righting moment, and by insufficient righting moment exerted by the horizontal tail surfaces. The problem has been solved by removing the strakes and by adding weight. Further tail redesign is not required to achieve towbody stability at speeds below ~90 knots.

(ii) Drag

The total drag was determined from photographs of the helicopter and towbody. Analysis of the photographs gave the position of the towbody relative to the helicopter. The curve of the tow rope could be seen clearly in the photographs, so it was possible to calculate the tow rope angle at the towbody. While an individual photograph gave very precise results for the tow rope angle, analysis of repeated runs showed that the tow-rope angle could be measured only with a standard deviation of ~1.1°. This provided the basic limit on the accuracy of the drag measurements. Smaller corrections were made for the effects of winglet and towbody lift in pitched-forward attitudes.

The total drag is calculated from the tow-rope angle θ and the towbody lift estimated from the IMD data :

$$\text{Drag} = \tan\theta \times (\text{Towbody weight} - \text{Lift}) \ . \qquad (6)$$

Fig. 6 presents the towbody drag coefficient calculated for a cross section of 0.61 m^2 for the first and third flights (winglets on, no strakes and winglets off, strakes on; the photographs from the second flight were lost and the videotape was not distinct enough to give accurate results). The uncertainty is dominated by the ±1.1° error in the tow rope angles. It appears that the drag coefficient is lower at the highest speeds, but the data are also consistent with a constant value of C_D~0.7.

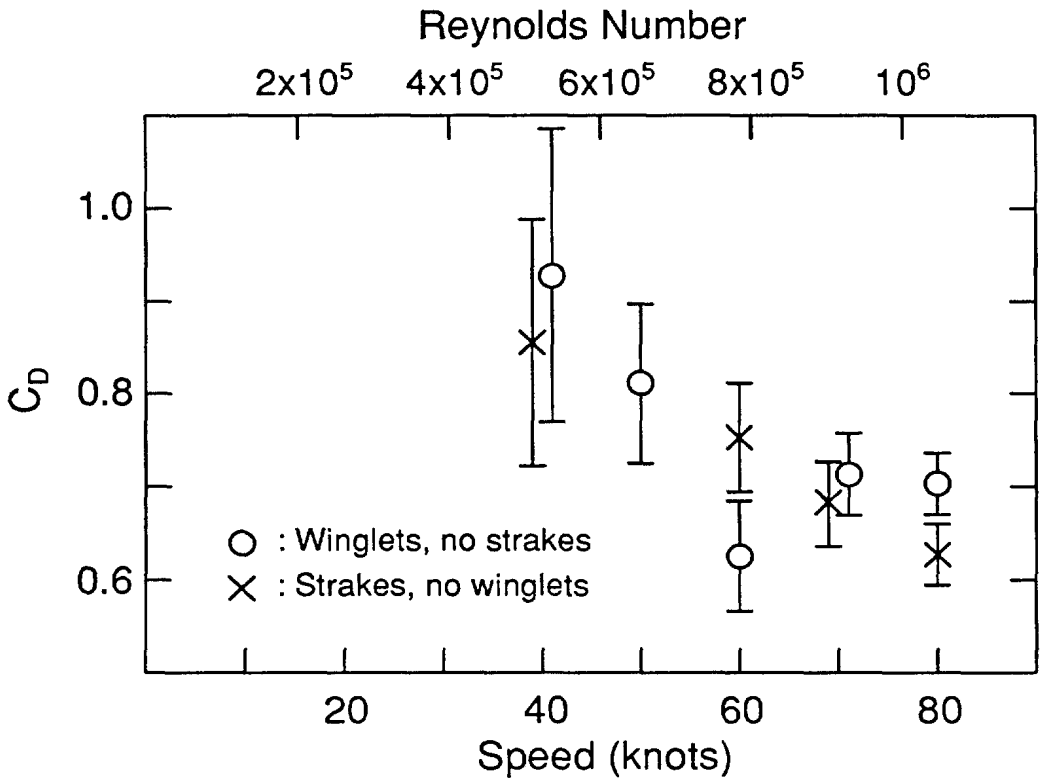

Figure 6. The drag coefficient of the towbody deduced from the tow-rope angles.

It is clear that the strakes added for the third flight increased the drag, at most, by a small amount, although they did increase the forward pitch. This suggests that the drag of the upper part of the towbody may have stayed constant or even decreased while the drag of the bottom rose.

The water-tank data reviewed in Section 2 indicated that the drag coefficient in the range 30-50 knots is constant at C_D=0.49 which is 30% less than the value C_D=0.7 derived from the flight tests. This is consistent with a calibration error in the water-tank data.

(iii) Tow-rope pendulum

In these trials, the towbody was carried on a 29-m tow rope. Consequently the towbody executes a pendulum motion around the cable attachment at the helicopter with frequency

$$f = \frac{1}{2\pi}\sqrt{\frac{T}{ML}} \qquad (7)$$

where T is the tow-rope tension, M is the towbody mass and L is the tow-rope length. The tow-rope tension is the vector sum of the towbody weight (214 lb, 952 N) and the aerodynamic drag (roughly $6.9\times10^{-2}\text{N}\times(\text{v/knot})^2$) giving pendulum frequencies ranging from 0.093 Hz at low speeds to 0.097 Hz at 80 knots.

Cross-power spectral analysis showed that the pendulum motions could be characterized as (i) a side-to-side motion, and (ii) a longitudinal/ pitching motion.

In the side-to-side pendulum motion, the towbody is forced to follow the air stream by the vertical tail surface, and this couples the roll and yaw motions. If the towbody is swinging from side to side with amplitude Y_0 while moving forward at speed v, then the roll and yaw are given by

$$\text{Roll} : \quad \rho(t) = \rho_0 \cos(\omega t)$$

$$\rho_0 = Y_0/L \tag{8}$$

$$\text{Yaw} : \quad \alpha(t) = \frac{\sqrt{gL}}{v} \times \rho_0 \sin(\omega t)$$

The powers and cross-power of the roll and yaw are

$$\text{Roll power} : \quad Q_{rr} = \rho_0^2 \tag{9a}$$

$$\text{Yaw power} : \quad Q_{yy} = \frac{gL}{v^2}\,\rho_0^2 \tag{9b}$$

$$\text{Cross-power} : \quad Q_{yr} = -i\,\frac{\sqrt{(gL)}}{v}\rho_0^2 \tag{9c}$$

The longitudinal pendulum motion produces a pitching signal at the pendulum frequency. We assume nothing about the coherence between the pitching and the coupled roll-yaw motion.

Power-spectral analysis of the magnetometer outputs gave the amplitudes of the roll, yaw and pitching motions and the results are shown in Fig. 7. It is hard to say much about the uncertainty in the amplitude estimates. In most cases, modelling the pendulum motion as two independent oscillations worked well, but the scatter in the results indicates that the results are accurate only to ~20% although the measurement uncertainty is much less than this. One problem is that the yaw axis is nearly vertical and so is the magnetic field at Cold Lake (dip angle=78°). Consequently, the magnetometer is quite insensitive to yaw motions particularly on some headings.

At speeds of 30 knots and greater, there is only a small pendulum motion and it is clear also that the winglets and strakes have a negligible effect on the amplitude of the 0.1-Hz motions of the towbody. At 20 knots, the yaw amplitude is in the range 4-10° (RMS) which results from a side-to-side motion of 3-8 m (peak-to-peak) assuming that the pendulum

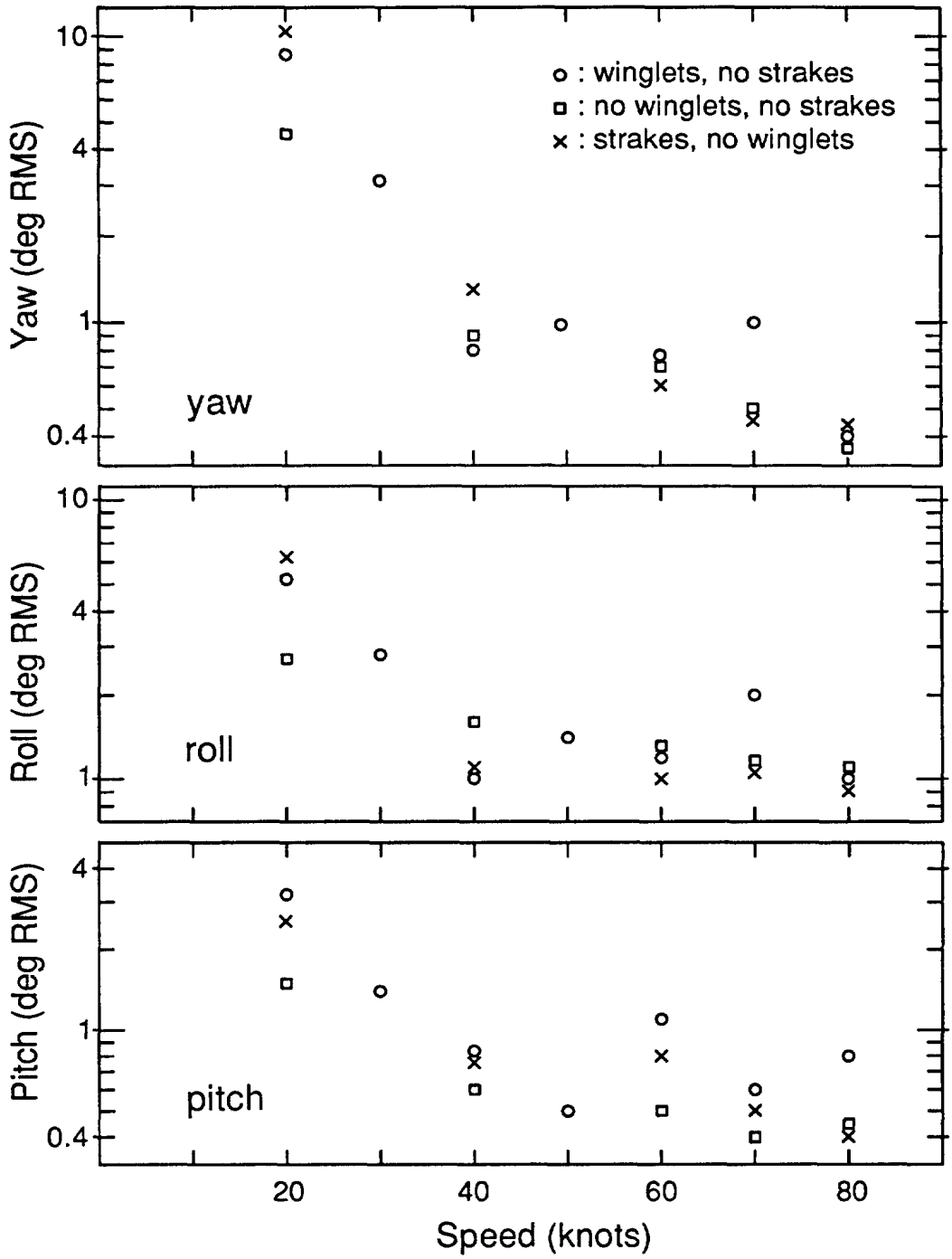

Figure 7. The amplitudes of the 0.1-Hz pendulum motions deduced from the magnetometer signals applying the model described in the text. The amplitudes are accurate to ~20%.

motion is a simple sinusoid. Inspection of the magnetometer signals shows that during the first two flights (no strakes, with and without winglets), there was no indication of an unstable increasing pendulum amplitude. In the third flight (with strakes and no winglets), the pendulum amplitude increased for the first 90 seconds of the 20-knot flight and then stayed roughly constant. This is not necessarily an indication of aerodynamic instability since the flight was performed in gusty conditions which could have excited the pendulum during the flight. Because there is no active yaw control in the towbody, the 0.1-Hz pendulum motion is not damped, and so once excited it tends to continue oscillating.

(iv) Acceleration spectra

Figure 8 shows power spectra of the accelerometer signals recorded during straight and level flight in the configuration with winglets removed and no strakes. The power spectra in the other configurations showed no significant differences, and there are no major differences between these spectra and the results presented in Ref. 1.

The peak at 1 Hz in the transverse acceleration is due to a side-to-side pendulum rocking of the towbody. Ref. 1 predicted that this rocking would appear at 1.2 Hz. The 0.65-Hz line in the forward acceleration is caused by free pitching around the point where the tow rope is attached to the towbody. The pitch and roll motions are discussed in part (v) of this section. The narrow lines at 5.4 and 10.8 Hz in the vertical acceleration are due to the main rotor of the helicopter which turns at 324 rpm and the broad line around 2 Hz is due to a spring action in the 6-mm diameter kevlar tow rope.

The 0.1-Hz tow-rope pendulum does not appear in the acceleration spectra. This follows from basic dynamics which shows that an accelerometer mounted at the centre of mass of a simple pendulum will show exactly zero lateral accelerations, and will show a component of acceleration along the pendulum at twice the pendulum frequency. Indeed a weak 0.2-Hz line does appear in the vertical accelerations.

The accelerations applied to the towbody are <0.04 g/$\sqrt{\text{Hz}}$ at all frequencies, and are <0.01 g/$\sqrt{\text{Hz}}$ except at the pitch and roll resonances. Most significantly, the acceleration noise is ~ 0.008 g/$\sqrt{\text{Hz}}$ in the frequency range 0.1-0.5 Hz which is most significant for ASW applications of MAD and it does not rise sharply with increasing air speed, at least for speeds up to 80 knots.

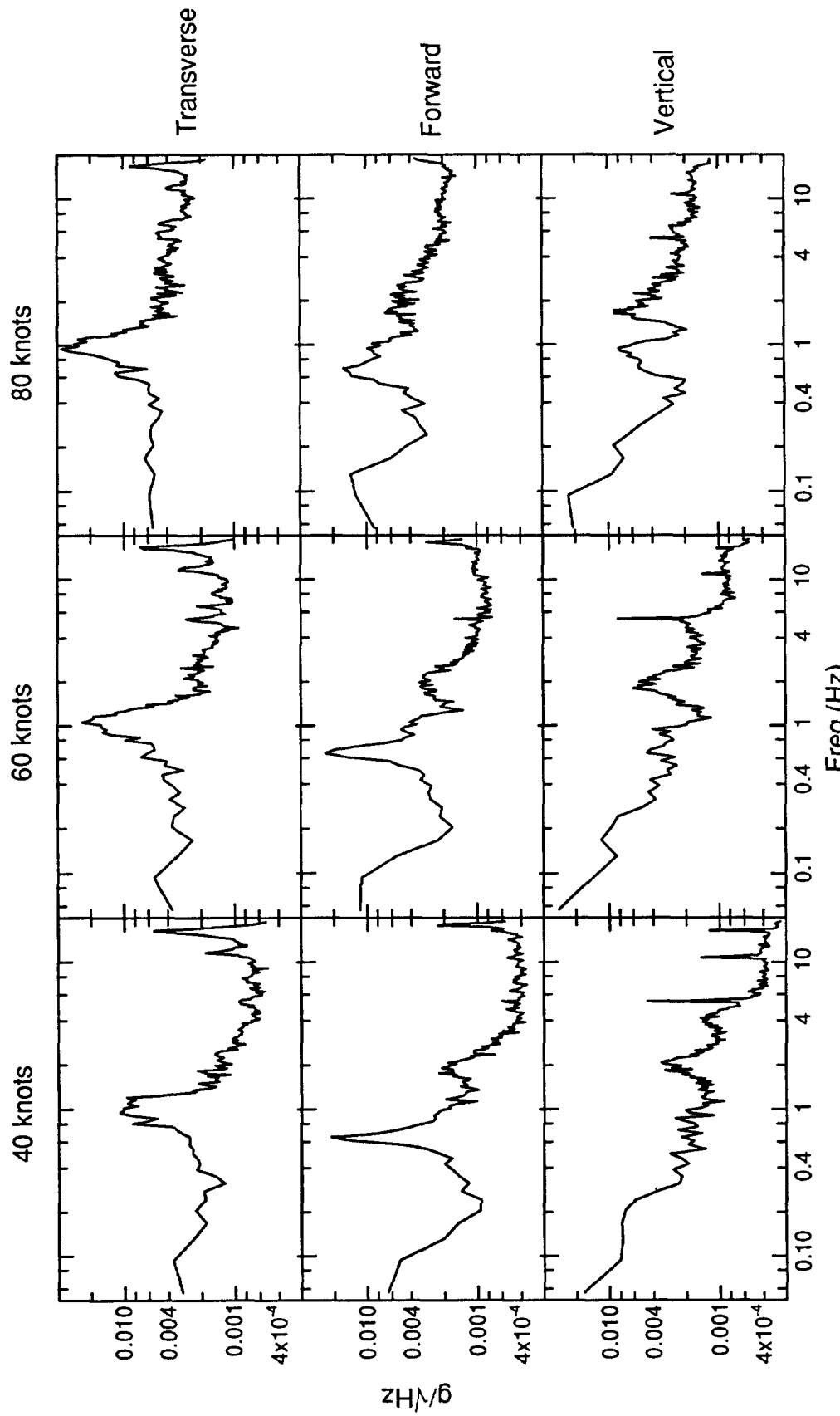

Figure 8. Acceleration spectra for the towbody with no winglets and no strakes in straight and level flight. Each spectrum is calculated from a 216-sec segment of data with a 26-sec cosine taper applied at each end. The spectra have been smoothed with δf=0.038 Hz for f<1.85 Hz and δf=0.02f for f>1.85 Hz.

(v) Pitch and roll motions

The towbody experiences short-period pitching and rolling motions which appear as clear peaks in the power spectra of the accelerometers and magnetometers (see Fig. 8). The short-period yaw is discussed in the next part of this section. The pitching motion is a simple pendulum motion about the tow point. The calculation based on towbody mass and moment of inertia predicted a pitching frequency of 0.5 Hz, but it actually appears at ~0.65 Hz. Since the pitch frequency is not speed dependent, the difference is not due to the fact that the tail and bottom plate provide a small additional restoring force which tends to increase the natural pitching frequency. A second motion appears as a side-to-side roll pendulum in which a restoring force provided by the tow-rope bridle adds the gravitational restoring force, thus increasing the natural frequency. Ref. 1, Appendix A predicted that the roll resonance would appear at 1.2 Hz, but both these data and ref. 1 show it at 0.9-1.0 Hz. Note that there is no connection between the side-to-side pendulum about the tow-rope attachment to the helicopter (0.1 Hz) and the high frequency roll motion.

Fig. 9 shows the measured pitch and roll amplitudes derived from the magnetometer signals. The rocking amplitudes tend to increase with air speed and do not exceed 0.35° (RMS) in roll and 0.65° (RMS) in pitch except for one flight at 60 knots. It is not clear why the data with winglets showed anomalous large rocking motion at 60 knots. There is no doubt that the towbody really did pitch and roll more at 60 knots during this flight, so it is not an error in the data analysis, but at the same time there does not seem to be a dynamical reason such as eddy shedding from the winglets. Note that the 0.65-Hz pitch and the 1-Hz roll amplitudes do not increase sharply with rising air speed for air speeds up to 80 knots.

In no case did the pitch or roll motion show any hint of the sort of instability observed during the first trial.

(vi) High-frequency yaw

The yawing motion that corresponds to the 0.65-Hz pitch and 1.0-Hz roll motions discussed in part (iv) has a speed-dependent frequency because the restoring force is provided by the lift of the vertical tail surfaces rather than gravity. The tail consists of two vertical surfaces measuring 14 cm ×96 cm. Ref. 4 (Chapter III) gives an expression for the lift coefficient C_L of a simple straight wing with angle of attack α :

$$C_L = \frac{2\pi\alpha}{\frac{1}{a} + \frac{2}{A}} \qquad (8)$$

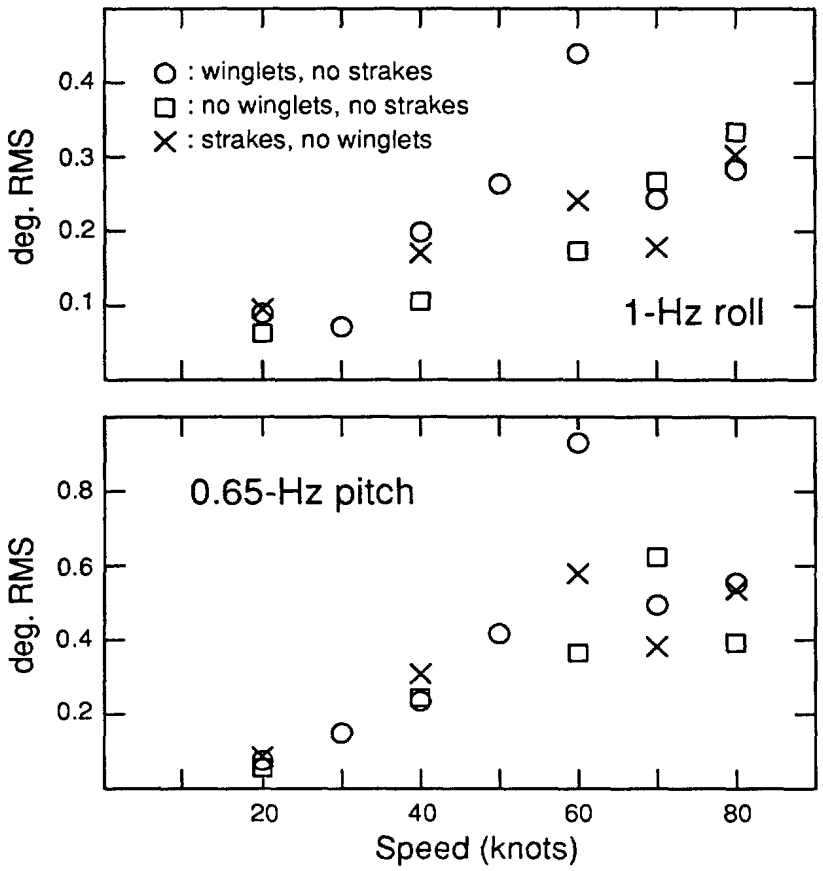

Figure 9. RMS roll and pitch amplitudes in straight and level flight derived from spectral analysis of magnetometer signals.

where A = aspect ratio (= 6.9 in this case) and Ref. 4 recommends a~0.9. With a total lifting surface area of S=0.27 m^2, the lateral force on the tail at airspeed v is

$$F_L = \frac{1}{2}\rho v^2 S C_L = K\alpha \ , \quad K=(0.21\ N/knot^2)\times v^2 \ . \tag{9a}$$

Since the tail force acts 0.46 m behind the towbody, the yawing moment is

$$M = J\alpha \ , \quad J=(0.095\ N\cdot m/knot^2)\times v^2 \ . \tag{9b}$$

The moment of inertia for rotations around the towbody's longitudinal axis is I_z = 2.55 $kg\cdot m^2$, giving a natural towbody-yaw frequency

$$f(yaw) = (0.031\ Hz/knot)\times v \ . \tag{10}$$

Equation (10) predicts that the natural yaw frequency increases from 1.5 Hz at 50 knots to 2.5 Hz at 80 knots.

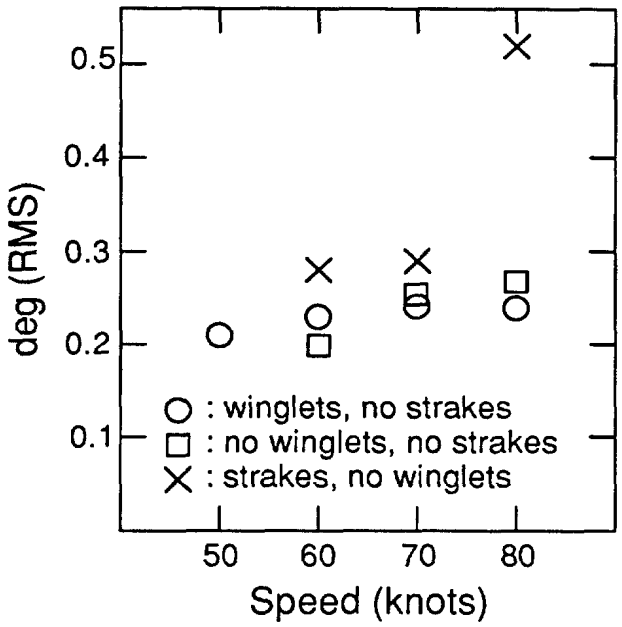

Figure 10. RMS yaw amplitudes deduced from spectral analysis of the transverse and forward magnetometer signals.

Analysis of the data showed that there was a weak yawing motion, and that it could be separated from the 1.0-Hz roll signal only at speeds above 50 knots. Figure 10 displays the yaw amplitudes deduced from power and cross-power spectral analysis of the transverse and forward magnetometer signals. These estimates are probably accurate to ±30%. There are no significant differences among the data from the three slightly-different towbody configurations except for the large yaw at 80 knots when the strakes were present. We do not know the source of the increased yaw in this case, but the third flight was done in gusty conditions and this may have increased the yaw amplitude.

The best estimates of yaw frequency are listed in Table II and they do not agree very well with the prediction given above. The yaw resonance is very broad, ~0.2 Hz, which indicates that the yaw motion is strongly damped, and it is hard to select the centre frequency. The fact that the resonant frequency is only ~75% of the predicted value indicates that the tail forces were significantly smaller than predicted. Fig. 1 shows that the tail's vertical surfaces were located 1.8×(towbody radius) to the side and should have experienced non-turbulent flow. However, if the tail surfaces were sitting in the towbody wake, then the yaw frequency would be reduced.

Table II. Measured and predicted yaw frequencies for the towbody. The yaw signal appeared as a very broad peak (FWHM~0.2 Hz) in the power and cross-power spectra of the magnetometer signals.

Speed (knots)	Yaw freq. (Hz)	Predicted freq. (Hz)
60	1.5	1.86
70	1.6	2.17
80	1.75	2.48

6. Conclusions

The flight test at AETE in November, 1993, demonstrated that the towbody developed by DREP is stable in flight up to 80 knots in level flight and in climbs and descents up to 1000 ft/min.

Analysis of the magnetometer and accelerometer signals shows that the towbody's pendulum and rocking motions are small enough that it can be used for a test of DREP's small superconducting gradiometer even without winglets to provide an additional righting moment. Strakes are unnecessary. The 14-kg weight added at the bottom of the towbody increased both the pitching moment of inertia and righting moment, and this was the principal reason for the improvement in the towbody's performance over the results reported in Ref. 1

The acceleration spectra show that the buffeting of the towbody in flight is <0.01 g/$\sqrt{\text{Hz}}$ except at spectral peaks due to small pitching and rolling motions of the towbody. This conclusion will be applied in the design of future gradiometers where the substrate design is selected so that sensor noise due to accelerations matches the sensor self-noise (see Refs. 5 and 6). The acceleration spectra, shown in Figure 8, do not increase sharply with increasing air speed for speeds up to 80 knots.

In the future, it may be necessary to reduce the pitch oscillation, which reached 0.9° (RMS) on one flight. This will require a new tail design in which a horizontal surface is mounted high enough that it is not in the turbulent air behind the towbody.

While the pitch, roll and yaw amplitudes are higher at higher air speeds, Figures 9 and 10 show that the increase is not a strong function of speed.

There is no indication of coupling between the aerodynamic forces on the towbody (ie. eddy shedding from the cylindrical body) and the side-to-side pendulum. This was a major concern in the design of the towbody and

was the reason that strakes were originally mounted on the towbody. If a more streamlined design is adopted in the future, the conclusion that there is no problem posed by the pendulum must be reviewed. While a streamlined shape would reduce the total drag, it would also result in a strong lateral force on a yawing towbody, and this could result in large-amplitude swings at low speeds.

Acknowledgements

Mr. Richard Religa of DREP designed and supervised construction of and modifications to the towbody. Because of his hard work, the towbody was ready for use well before both flight trials and the water-tank test at IMD.

The staff at AETE made the flight trials possible. Capt. M. Lacroix coordinated both trials, and Capt. S. Carrignan flew the CH-135 helicopter in both cases. We are particularly grateful for the takeoffs and landings which were difficult, but which were performed without damage to the towbody. The careful control of the helicopter during 5-min straight and level flights at speeds ranging from 20 to 80 knots elicited the admiration of his copilot, Capt. Fidele, and the chase-helicopter pilot, Capt. Erdos. The long straight and level flights permitted a detailed spectral analysis of accelerometer and magnetometer signals. The AETE photography section provided us with detailed photographs and videotapes of the flights.

References

1. Hopkin, D. and H. Wilson, "Design and Test of a Towbody for an Airborne SQUID Gradiometer", DREP Technical Memorandum 92-44, October 1992

2. Schlichting, H., Boundary-Layer Theory, 7th edition, McGraw-Hill 1979

3. Goldstein, S., Modern Developments in Fluid Dynamics, Oxford University Press, 1938 p. 439

4. Hoerner, S. and H. Borst, Fluid-Dynamic Lift, Hoerner Fluid Dynamics 1985

5. Betts, K. et al., "Investigation and Design of a Superconducting Magnetic Gradiometer", DREP Contractor's Report 92-27

6. Wilson, H., "The Status of Superconducting Magnetic Gradiometer Development at DREP", DREP Technical Memorandum 93-27, March 1993

DISTRIBUTION

REPORT : Technical Memorandum 94-16

TITLE : Flight Test of a Cylindrical Towbody for an Airborne SQUID Gradiometer

AUTHORS : Harold Wilson, David Hopkin, Brian Dunstan and J. Bradley Nelson

DATE : March 1994

SECURITY : Unclassified

Dept. of National Defence

DREP	6 copies
DREO	1
DREA	1
NDHQ - CRAD	1
DRDA	2
DMA	1
DSIS	2
DMAEM-4-2-9	2
DAS Eng 6-4	2
CFB Cold Lake	
AETE/FTA	2

External

Institute for Marine Dynamics 1
P.O. Box 12093, Postal Stn. A
St. John's, Nfld.
A1B 3T5

CTF Systems, Inc. 1
15-1750 McLean Ave.
Port Coquitlam, B.C.
V3C 1M9
Attn. : Dr., Jiri Vrba

UNCLASSIFIED

SECURITY CLASSIFICATION OF FORM
(highest classification of Title, Abstract, Keywords)

DOCUMENT CONTROL DATA

(Security classification of title, body of abstract and indexing annotation must be entered when the overall document is classified)

1 ORIGINATOR (the name and address of the organization preparing the document Organizations for whom the document was prepared, e g Establishment sponsoring a contractor's report, or tasking agency, are entered in section 8.)

Defence Research Establishment Pacific

2. SECURITY CLASSIFICATION (overall security classification of the document including special warning terms if applicable)

Unclassified

3 TITLE (the complete document title as indicated on the title page. Its classification should be indicated by the appropriate abbreviation (S,C or U) in parentheses after the title.)

Flight Test of a Cylindrical Towbody for an Airborne SQUID Gradiometer

4 AUTHORS (Last name, first name, middle initial)

Wilson, Harold S. /Hopkin, David A. /Dunstan, Brian W. /Nelson, J. Bradley

5 DATE OF PUBLICATION (month and year of publication of document)	6a NO. OF PAGES (total containing information Include Annexes, Appendices, etc.)	6b NO OF REFS (total cited in document)
March 1994	21	5

7 DESCRIPTIVE NOTES (the category of the document, e.g technical report, technical note or memorandum If appropriate, enter the type of report e g interim progress, summary, annual or final Give the inclusive dates when a specific reporting period is covered.)

Technical Memorandum

8 SPONSORING ACTIVITY (the name of the department project office or laboratory sponsoring the research and development Include the address.)

DREP

9a PROJECT [redacted] (if appropriate, the applicable research and development project or grant number under which the document was written. Please specify whether project or grant)	9b CONTRACT NO (if appropriate, the applicable number under which the document was written)
37A02	

10a ORIGINATOR'S DOCUMENT NUMBER (the official document number by which the document is identified by the originating activity This number must be unique to this document.)	10b OTHER DOCUMENT NOS (Any other numbers which may be assigned this document either by the originator or by the sponsor)
DREP Tech Memo 94-16	

11 DOCUMENT AVAILABILITY (any limitations on further dissemination of the document, other than those imposed by security classification)

(X) Unlimited distribution
( ) Distribution limited to defence departments and defence contractors, further distribution only as approved
( ) Distribution limited to defence departments and Canadian defence contractors; further distribution only as approved
( ) Distribution limited to government departments and agencies; further distribution only as approved
( ) Distribution limited to defence departments; further distribution only as approved
( ) Other (please specify):

12 DOCUMENT ANNOUNCEMENT (any limitation to the bibliographic announcement of this document This will normally correspond to the Document Availability (11) However, where further distribution (beyond the audience specified in 11) is possible, a wider announcement audience may be selected.)

Unlimited

UNCLASSIFIED

SECURITY CLASSIFICATION OF FORM

DCD03 2/06/87

13 ABSTRACT (a brief and factual summary of the document. It may also appear elsewhere in the body of the document itself. It is highly desirable that the abstract of classified documents be unclassified. Each paragraph of the abstract shall begin with an indication of the security classification of the information in the paragraph (unless the document itself is unclassified) represented as (S), (C), or (U). It is not necessary to include here abstracts in both offical languages unless the text is bilingual.)

The Magnetic Anomaly Detection Group at DREP is studying the feasibility of using SQUID magnetic gradiometers in airborne antisubmarine warfare. As part of this project, a non-magnetic towbody has been built to carry a vertical gradiometer in an airborne trial of SQUID systems. The towbody is essentially a circular cylinder with the air flow perpendicular to the cylinder axis. We describe the characteristics of the towbody that were observed during a flight test. The results presented include drag, static pitch, towbody oscillations and acceleration spectra. We conclude that the towbody can be used for a trial of a gradiometer.

14 KEYWORDS, DESCRIPTORS or IDENTIFIERS (technically meaningful terms or short phrases that characterize a document and could be helpful in cataloguing the document. They should be selected so that no security classification is required. Identifiers, such as equipment model designation, trade name, military project code name, geographic location may also be included. If possible keywords should be selected from a published thesaurus, e.g. Thesaurus of Engineering and Scientific Terms (TEST) and that thesaurus-identified. If it is not possible to select indexing terms which are Unclassified, the classification of each should be indicated as with the title.)

Aerodynamics
Towbody
Cylinder